ACS APPLIED MATERIALS & INTERFACES

Research Article

www.acsami.org

Galactose Targeted pH-Responsive Copolymer Conjugated with Near Infrared Fluorescence Probe for Imaging of Intelligent Drug Delivery

Liyi Fu,[†] Chunyang Sun,[‡] and Lifeng Yan*,[†]

[†]CAS Key Laboratory of Soft Matter Chemistry, Hefei National Laboratory for Physical Sciences at the Microscale, Collaborative Innovation Center of Chemistry for Energy Materials, and Department of Chemical Physics and [‡]School of Life Sciences, University of Science and Technology of China, Hefei, 230026, P.R. China

Supporting Information

ABSTRACT: Theranostic polymeric nanomaterials are of special important in cancer treatment. Here, novel galactose targeted pH-responsive amphiphilic multiblock copolymer conjugated with both drug and near-infrared fluorescence (NIR) probe has been designed and prepared by a four-steps process: (1) ring-opening polymerization (ROP) of *N*-carboxy anhydride (NCA) monomers using propargylamine as initiator; (2) reversible addition−fragmentation chain transfer (RAFT) polymerization of oligo(ethylene glycol) methacrylate (OEGMA) and gal monomer by an azido modified RAFT agent; (3) combing the obtained two polymeric segments by click reaction; (4) NIR copolymer prodrug was synthesized by chemical linkage of both cyanine dye and anticancer drug doxorubicin to the block copolymer via amide bond and hydrazone, respectively. The obtained NIRF copolymers were characterized by nuclear magnetic resonance (NMR), gel permeation chromatography (GPC), and its was measured by means of micelles dynamic light scattering (DLS), field emission transmission electron microscopy (FETEM), and UV−vis and fluorescence spectrophotometry. The prodrug has strong fluorescence in the near-infrared region, and a pH sensitive drug release was confirmed at pH of 5.4 via an in vitro drug release experiment. Confocal laser scanning microscopy (CLSM) and flow cytometry experiments of the prodrug on both HepG2 and NIH3T3 cells reveal that the galactose targeted polymeric prodrug shows a fast and enhanced endocytosis due to the specific interaction for HepG2 cells, indicating the as-prepared polymer is a candidate for theranosis of liver cancer.

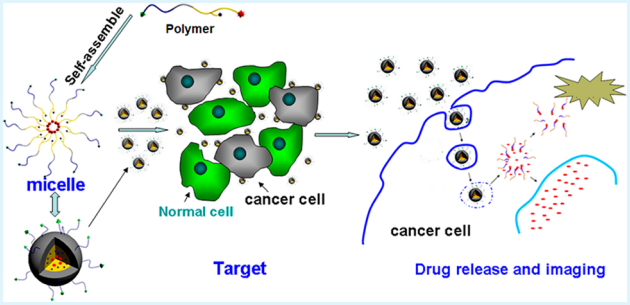

KEYWORDS: *theranostic, near-infrared (NIR), amphiphilic copolymer, fluorescence, pH-responsive*

INTRODUCTION

Targeting and stimuli-responsive drug delivery is specially important and interesting, which has attracted much attention recently.[1,2] Plenty of novel polymers or nanoparticles with those functions have been synthesized as the carriers for drugs.[3,4] However, information with less detail of the endocytosis of the drug delivery system (DDS) and the fate of both the drug and its carriers especially targeted the accumulation of DDS to the cancer cells or tissue. If an "eye" is conjugated to the system, it will efficiently promote the understanding of the interaction of DDS with cell and the targeting process, especially the key information on the process in the drug delivery inside cells.[5−8] So the combination of drug delivery and imaging is very important for developing new theranostic agents.[9,10]

Imaging of the cancer cells or tumor at the early stage is vital, and various methods for tumor imaging based on imaging modalities have been developed recently,[11,12] such as metallic or magnetic radioisotopes for positron emission tomography (PET),[13] nanoparticles for magnetic resonance imaging (MRI),[14,15] or quantum dots[16−18] and organic fluorescent dyes[19−21] for optical imaging. Recently, imaging in the near-infrared region (700−900 nm), which can eliminate the undesired background noises, becomes a more valid method for both in vivo and in vivo imaging.[22−29]

The development of intelligent DDS[30−33] with environmental stimuli responsive release is attractive. Both physical[34,35] or/and chemical methods have been applied,[36−38] while reduction[39,40] or pH-responsive release[34,38] are the two mostly utilized stimuli methods. It is well-known that the tumor cell is more acidic,[41] and the chemical bond cleavage under acid conditions could trigger the release of the conjugated drug.[42] Hydrazone bonds between the drug and the polymeric carrier are the ideal linkage for the pH-responsive release of the carrier drug.[37,43]

The treatment of liver cancer is an emergency task in Asia. By now, it is still a challenge to image the target drug delivery process in cells or tumors.[44−47] Specific tumors could be targeted by nanoparticles with different functional groups via the ligand−receptor-recognition,[48,49] and targeting ligands

Received: November 27, 2014
Accepted: January 8, 2015
Published: January 8, 2015

DOI: 10.1021/am508291k
ACS Appl. Mater. Interfaces 2015, 7, 2104−2115

Scheme 1. Structure of Ligand Targeted Copolymer Conjugated with DOX and NIR Probe, Micellization, Selective Accumulation in Liver Cancer Cell, and Imaging of the Endocytosis of the Micelle with Subsequent pH Triggered Drug Release

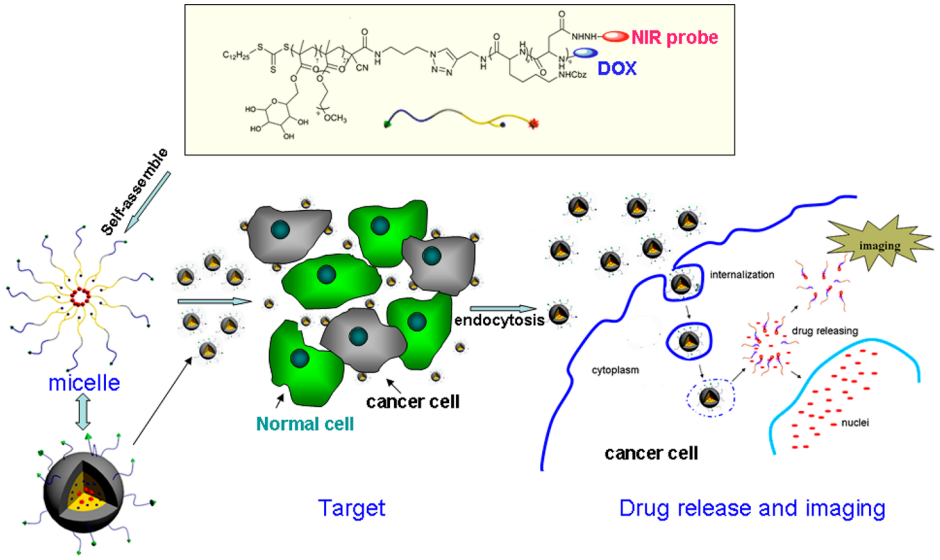

include folic acid,[50−52] antibody,[53,54] peptide,[55−57] and galactose/lactose.[58−61] Galactose functionalized polymer has been widely utilized as a biomedical material for drug delivery for liver cancer for HepG2 cell overexpresses galactose receptor asialogly coprotein (ASGP-R).[62,63] The combination of target ligand galactose, NIRF cyanine dye, and responsive drug into one polymeric chain will be a useful method for imaging of liver cancer and tumor theranosis.

Here, a novel multiblock copolymer has been designed and synthesized base on the ROP polymerization of *N*-carboxy anhydride (NCA) monomers. Considering the low solubility of the amino acids such as aspartic acid, it is necessary to introduce hydrophilic groups such as polyethylene glycol (PEG) to constitute the amphiphilic molecules. Oligo(ethylene glycol) methacrylate (OEGMA) was used as one monomer to be polymerized by means of reversible addition−fragmentation chain transfer (RAFT) polymerization, and the target ligand was conjugated to the chain using RAFT polymerization of galactose containing monomer Gal (Scheme 1). Three kinds of copolymers with the NIR probe, namely, targeting copolymers (TCs), nontargeting copolymers (NCs), and copolymers without drugs (CWDs) have been synthesized, and their drug delivery behaviors for both HepG2 and NIT3H3 cell were studied.

RESULTS AND DISCUSSION

Synthesis of Functional Triblock Copolymer by Combination of RAFT, ROP, and Click Reaction. Ring-opening polymerization (ROP) and radical polymerization are two common methods which are widely used on polymer synthesis while the primary amine groups were often used for the ring-opening polymerization of *N*-carboxy anhydride (NCA) monomers for polypeptides.[64] However, it is difficult to insert the PEG chain or other functional groups like targeted ligand into the polypeptide chains. In addition, the RAFT agent is a very good initiator for radical polymerization. Therefore, the design of a primary amine group-containing RAFT agent is hopeful for combination of the RAFT and ROP methods to prepare multifunctional polymers.[27,28] However, found by previous experiments, the thioester bond of the RAFT agents is unstable to the primary amine group, so the amine group is always protected by trifluoroacetic acid if it is linked to the agents. Moreover, it had been reported that RAFT agents containing a cyano group have a higher activity to which MAlpGP monomer can be polymerized. However, because of the fact that the cyano group can be hydrolyzed in acid conditions and this method is not suitable for this system. So our strategy is using a three-steps process to synthesize the targeted PEGalated amphiphilic copolymer: (1) ring-opening polymerization (ROP) of *N*-carboxy anhydride (NCA) monomers using propargylamine as the initiator; (2) reversible addition−fragmentation chain transfer (RAFT) polymerization of oligo(ethylene glycol) methacrylate (OEGMA) and gal monomer by an azido modified RAFT agent; (3) combing the obtained two polymeric segments by click reaction.

To the copolymer, the DOX and NIR probe were conjugated to the chains by covalent bonds. Considering the character of hypotoxicity and high biodegradability of aspartic acid, we choose it as the binding sites of the hydrazine bond. In addition, lysine has been found in our previous studies with an enhancement in fluorescence of cyanine dye to some extent.[65] So derivatives of these two amino acids, to which doxorubicin and cyanine dyes were linked, were selected to form the hydrophobic part of the copolymer.

Since HepG2 cell overexpresses asialogly coprotein (ASGP-R) on its surface, galactose conjugated polymers could be selectively uptook by HepG2 cell via the ligand−receptor-recognition process.[62,63] Here, RAFT polymerization of MAlpGP monomer was used to induce galactose targeted ligand to the copolymer.

Synthesis of RAFT-APA. At first, a RAFT agent containing a cyano group was synthesized, and the ^{1}H NMR spectrum of the RAFT agent was shown in Figure S1a in the Supporting Information. The three hydrogen atoms were selected as the standard to standardize the peak integrations. The hydrogen atoms from the second to the tenth carbon atom from the terminal group had the same chemical shifts, so they were all marked as hydrogen *b*. Except hydrogen *e*, other integration of the peaks nearly corresponded to the number of hydrogen atoms. It may be that the spin of the hydrogen *e* was influenced

DOI: 10.1021/am508291k
ACS Appl. Mater. Interfaces 2015, 7, 2104−2115

Scheme 2. Synthesis of the Targeting, Amphiphilic, Near-IR and pH-Responsive Triblock Copolymer via Radical and Ring-Open Polymerization

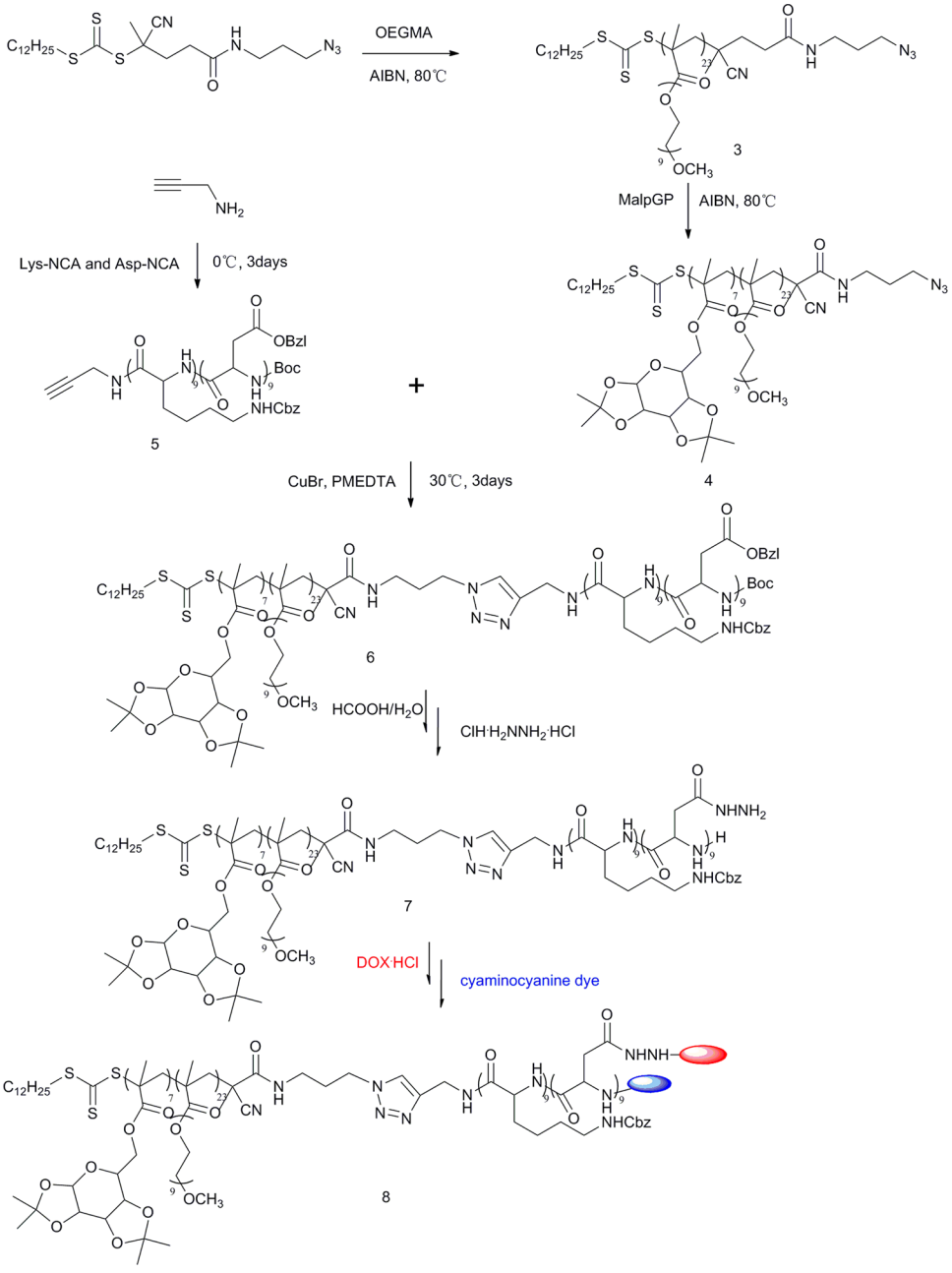

by the steric hindrance or some other reasons. The coupling constant of hydrogen *b* could not be measured because the amounts of hydrogen atoms had similar chemical shifts. Figure S1b in the Supporting Information shows the typical ^{1}H NMR of APA, and clearly highly pure APA was prepared. Figure S1c in the Supporting Information shows the ^{1}H NMR spectrum of RAFT-APA, and all the peaks can be well assigned to the corresponding hydrogen in the molecule. On the other side, the FT-IR spectra (Figure S1d in the Supporting Information) of the compound clearly shows the peak of 2096 cm^{-1} which belongs to the azido group.

Synthesis of Polymer APA-RAFT-POEGMA. The ^{1}H NMR spectrum of APA-RAFT-POGEMA was shown in Figure S2 in the Supporting Information. Because of the large molecule weight of the polymer, many peaks overlapped and could not be distinguished. Characteristic chemical shift of the OEGMA could be observed at 4.18 ppm for hydrogen *f*, which is the first two hydrogen atoms near the ester group. Integration of peak *f* to *a* is about 46:3, indicating that approximately 23 units of OEGMA were polymerized to the RAFT agent.

Synthesis of APA-RAFT-PMalpGP-*b*-POEGMA. Similar to the spectrum of APA-RAFT-POEGMA, many peaks overlapped so that not every hydrogen atom could be corresponding to the peaks. Characteristic chemical shifts of the MalpGP could be observed at 5.50 and 4.61 ppm for hydrogen *b* and *c*, respectively. Integration of peak *b* and *c* to *a* are about 7:1, indicating that approximately 7 units of MalpGP were polymerized to the RAFT agent (Figure S3 in the Supporting Information).

DOI: 10.1021/am508291k
ACS Appl. Mater. Interfaces 2015, 7, 2104−2115

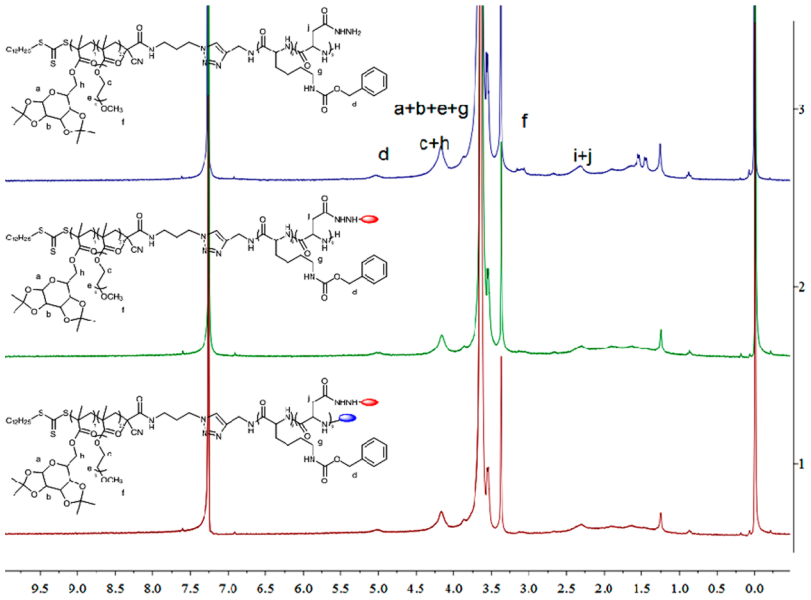

Figure 1. ^{1}H NMR spectrum of PMalGP-*b*-POEGMA-*b*-P(Llys-*co*-(Asp-NHNH$_2$)) (curve 1), the copolymer conjugated with DOX (curve 2), and the copolymer conjugated with both DOX and NIR probe (curve 3) in $CDCl_3$.

Synthesis of PA-P(Llys-*co*-Asp)-Boc. The segment of polypeptide was synthesized by ROP polymerization of LLys-NCA and Asp-NCA sequentially using propargylamine as initiator at low temperature. Figure S4 in the Supporting Information shows the ^{1}H NMR spectrum of the product, and characteristic chemical shifts of the propargylamine could be observed at 3.84 ppm for hydrogen *b*, while the Llys at about 5 and 3.08 ppm for hydrogen *l* and *g*, respectively, and the Asp at about 5 ppm. The integration ratio of peak *b* to *g* is 2:18.56, indicating approximately 9 units of Llys were polymerized to the propargylamine. Similarly, the ratio of peak *b* to *j* + *l* is 2:36, indicating the sum of Llys and Asp units is about 18. Approximately, 9 units of Asp were linked.

Synthesis of PMalpGP-*b*-POEGMA-*b*-P(Llys-*co*-Asp). The click reaction was used to combine the as-prepared two polymeric segments as shown in Scheme 2. Figure S5 in the Supporting Information shows the ^{1}H NMR spectrum of the copolymer after the click reaction. Characteristic chemical shifts of the MalpGP could be observed at 5.50 and 4.61 ppm for hydrogen *b* and *a*, respectively. Integration of peak *b* to *c* + *d* is about 7:38, indicating that the ratio of the hydrophilic diblock polymer APA-RAFT-PMalpGP-POEGMA linked to hydrophobiccopolymer PA-P(Llys-*co*-Asp) was 1:1. The disappearance of the 2096 cm^{-1} which was shown in the FT-IR spectrum (Figure S6 in the Supporting Information) illustrated the completed consumption of the azido group, indicating the efficient combination of the hydrophilic and hydrophobic parts.

Deprotection of the MalpGP. Deprotection of the copolymer did not bring much change to the molecule structure so that the spectrum was similar to the spectrum of PMalpGP-*b*-POEGMA-*b*-P(Llys-*co*-Asp)-Boc. The disappearance of the peaks at 5.50 and 4.61 ppm and the decreasing of the peaks at about 1.4 ppm illustrated the deprotection of galactose and the Boc group (Figure S7 in the Supporting Information).

Synthesis of Cyanine Dye. To conjugate Cy7,5 like dye to the polymer, a terminal carboxyl group cyanine dye was synthesized, and Figure S8 in the Supporting Information shows its ^{1}H NMR spectrum. Obviously, the target molecule was obtained with high purity.

Synthesis of Drug and Cyanine Dye Conjugated Triblock Copolymer. In this step, hydrazine group displaced benzyloxy group which was on Asp. The ratio of *d* to *a* changed from 36:3 to 18:3, indicating that the progress of hydrazinolys is finished (Figure 1). After the reaction of the carboxyl group of dyes and the terminal amine group of the copolymer, a cyanine dye conjugated copolymer was obtained. Owing to the fact that one molecule of doxorubicin and one-tenth a molecule of cyanine dye were added to the copolymer, respectively, and many peaks overlapped, the ^{1}H NMR spectra of the final copolymer did not change much more (Figure 1). Figure S9 in the Supporting Information shows the FT-IR spectra of the as-prepared copolymer conjugated with both the DOX and NIR probe, and the presence of DOX in the copolymer was evident from the observed bands at 1260−1000 and 860 cm^{-1}. The presence of the NIR probe is indicated by the observed bands at 1532 and 753 cm^{-1}.

In order to make clear the molecular structure of the final product, GPC traces of a series of intermediates and the final product were measured, and Figure 2 shows the results. Both RI and fluorescence detectors were used to characterize the products. A shift toward lower elution time (corresponding to higher molecular weight) was observed as the monomers were polymerized to the initiator. As shown in Figure 2a, the diblock polymer APA-RAFT-PMalpGP-*b*-POEGMA had a little higher molecule weight than the APA-RAFT-POEGMA, due to the fact only several units of MalpGP were added to the polymer which was less compared to the units of OEGMA. All the peaks in the image were single without any shoulder peak, indicating a well controlled polymerization. After the Click reaction, a less retaining time peak was measured without any residual peak at the elution time of the two reactants, illustrating that both the diblock polymer APA-RAFT-PMalpGP-*b*-POEGMA and the copolymer PA-P(Llys-*co*-Asp)-Boc were completely reacted. After conjugation with DOX and the cyanine dye, the GPC trace (curve 1 in Figure 2b) shows little change compared to its mother copolymer, and it is difficult to say the final target

DOI: 10.1021/am508291k
ACS Appl. Mater. Interfaces 2015, 7, 2104−2115

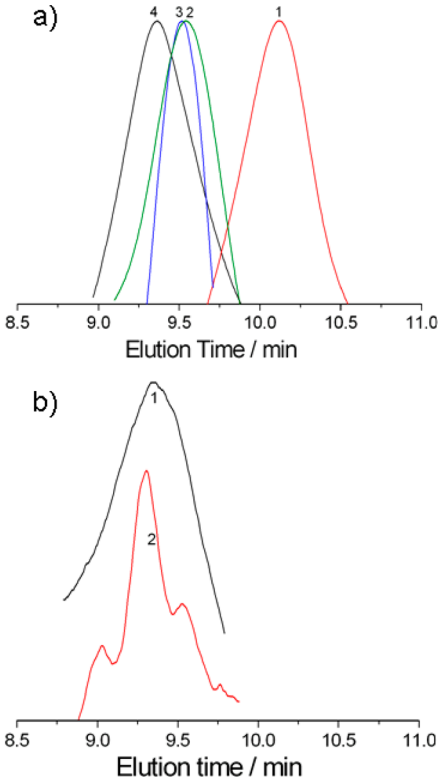

Figure 2. (a) GPC traces of PA-P(Llys-*co*-Asp)-Boc (1), APA-RAFT-POEGMA (2), APA-RAFT-PMalpGP-*b*-POEGMA (3), and PMalpGP-*b*-POEGMA-*b*-P(Llys-*co*-Asp)-Boc (4) in DMF measured by the RI detector; (b) GPC traces of the final polymer by means of RI detector (1) and fluorescence detector (curve 2, Ex@650 nm and Em@795 nm).

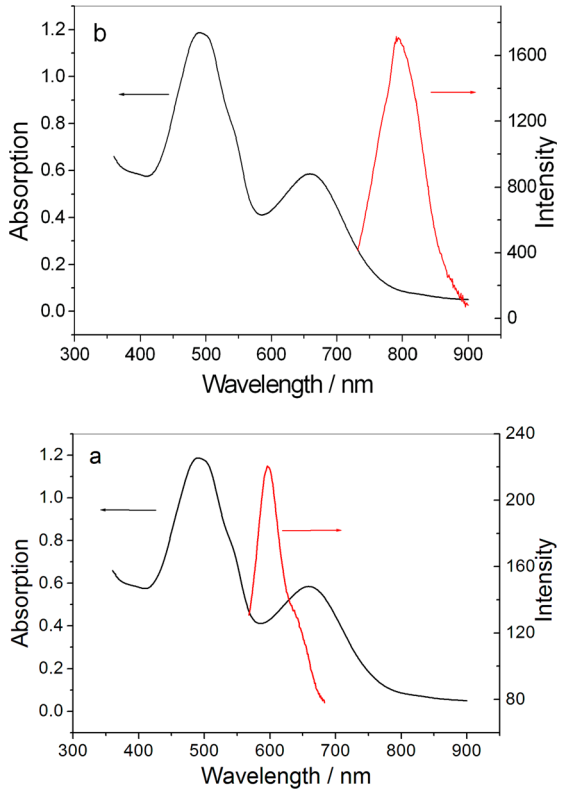

Figure 3. Absorption (black solid line) and emission (red dashed line) curves of the TC micelle solution (a) excited at 480 nm and (b) excited at 650 nm. The excitation and emission slit widths were 5 and 10 nm, respectively.

polymer was synthesized successfully. In order to make clear whether the target conjugated copolymer was obtained, the fluorescence detector of GPC was used at the same time, and as shown in Figure 2b, curve 2 is the GPC trace of the copolymer with 795 nm fluorescence emission wavelengths. Clearly, the target conjugated copolymer has been successfully prepared by covalent bonds as shown in Scheme 2. In addition, the curve 2 in Figure 2b shows shoulder peaks, indicating the wide distribution of the molecular weight of the polymer, and the fluorescence detector is in higher resolution than the RI detector.

Optical Properties of the Copolymer. Figure 3 shows the UV−vis and fluorescent spectra of the polymeric prodrug dispersed in water. Two peaks of 480 and 650 nm could be observed for the drug and dye segments while 597 and 795 nm correspond to the emission peaks of them, respectively. Fluorescence intensity of the cyanine dye is approximately 1600, indicating its high fluorescence property, and the quantum yield is about 1%, higher than the other cyanine dyes used in our groups.

Morphological Characterization. TEM and DLS were used to measure the size and size distribution of the polymeric prodrug micelle. The results are shown in Figure 4. All the micelles are in narrow size distribution with a size around 95, 85, and 93 nm for TC, NC, and CWD, respectively. The zeta potential of the conjugates has been also measured, and they are −25.3, −26.5, and −25.4 for TC, NC, and CWD, respectively, indicating the negative charge properties of the nanoparticles.

Drug Release. Both acidic (pH = 5.4) and neutral (pH = 7.2) conditions were utilized to study the in vitro pH-responsive drug release behavior of the polymeric prodrug, respectively. As shown in Figure 5 in the first 20 h, drug release was slow under neutral conditions, and for 52 h, it was still slow and less than 31% for the total drug release in 72 h. However, an obvious acid promoted drug release behavior was observed under acidic conditions, and the total drug release is up to 65% in 72 h. The cleavage of hydrazone bond under acidic conditions leads to the accelerated release of conjugated drug, indicating the prodrug is pH-responsive.

Cytotoxicity. The MTT method has been utilized to study the cytotoxicity of the TCs against the HepG2 and NIH3T3 cell in vitro, respectively. Toxicity of NCs and CWDs was also evaluated. Maintaining a consistent concentration of the doxorubicin in the copolymer, the cell survival ratio was evaluated under different concentrations, while the concentration of CWDs was kept the same as the TCs. Figure 6a,b shows the results. In both cells, more than 90% cells incubated with CWDs were still alive. In NIH3T3 cells, the mortality of the cells incubated with TCs and NCs is almost the same, which increased to nearly 70% when the concentration was added to 20 μg/mL, and diversely this ratio produced a difference in HepG2 cells. For the same concentration of polymer, cells incubated with TCs obviously had higher mortality than the cells incubated with nontarget ones. Because of the fact that CWDs have low toxicity, the mortality depends on the concentration of the doxorubicin which was released to the cells. From the results given above, it can be concluded that TCs have higher selectivity to HepG2 cells due to the conjugation of the MAlpGP ligand. With the same concen-

DOI: 10.1021/am508291k
ACS Appl. Mater. Interfaces 2015, 7, 2104−2115

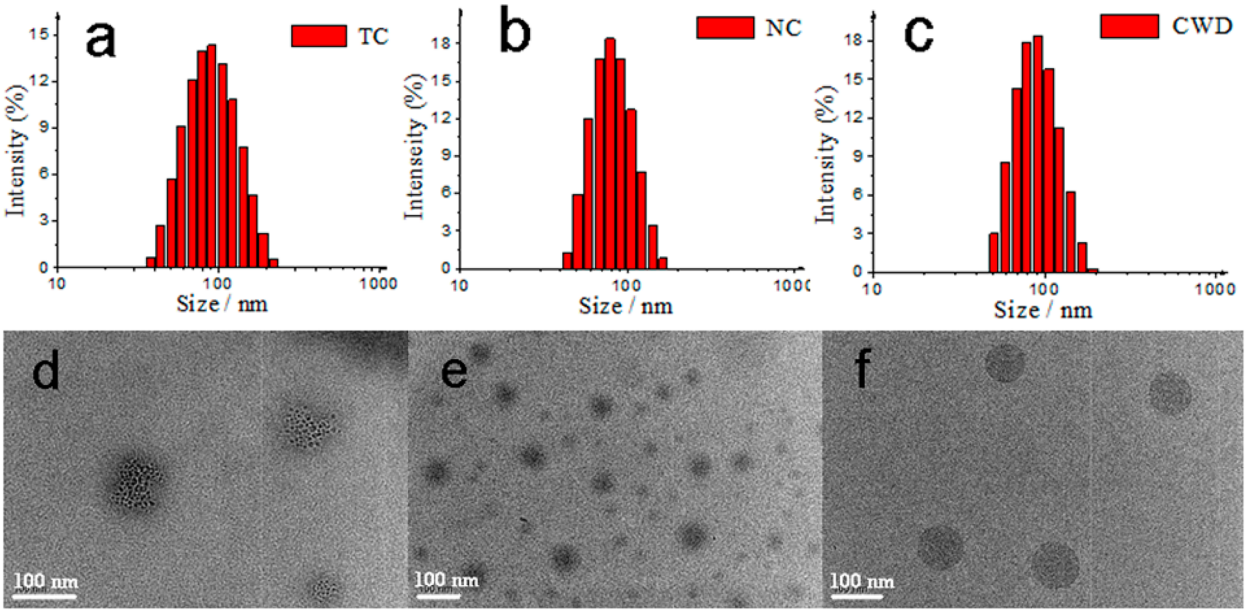

Figure 4. Size and size distribution of TC (a and d), NC (b and e), and CWD (c and f) solution determined by DLS and FETEM.

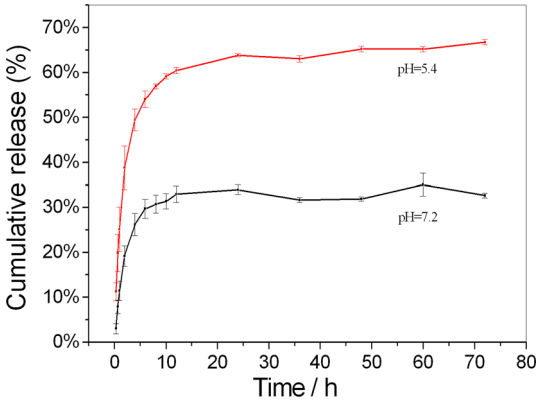

Figure 5. Drug release behavior of the target copolymers under neutral (pH = 7.2) and acidic (pH = 5.4) conditions.

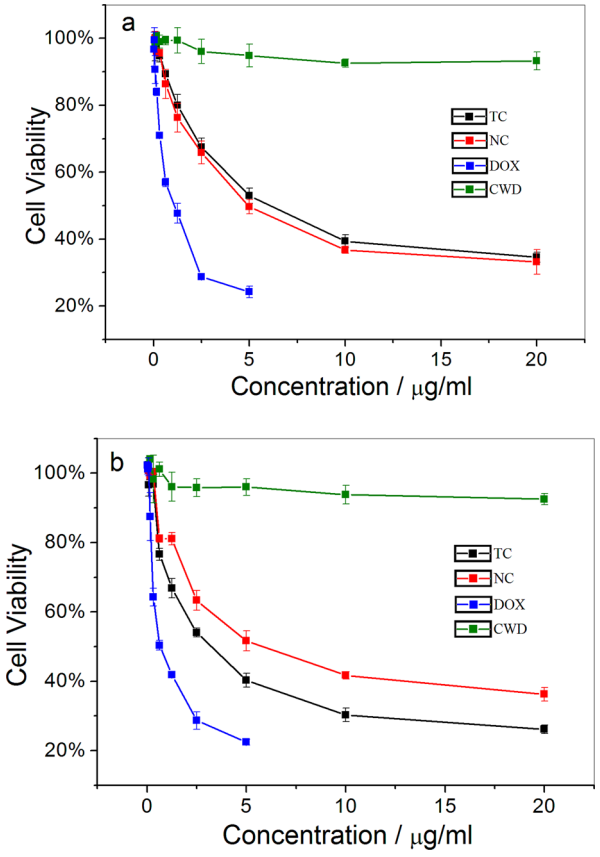

Figure 6. Cytotoxicity of free DOX (blue), TC (black), NC (red), and CWD (green) in (a) NIT3H3 cells and (b) HepG2 cells.

tration of the drug, free DOX can directly act on the cells. Otherwise, the copolymers with drugs would slowly release DOX to the cells and not all but some of them were released. So the mortality of the copolymers was lower than free DOX. In addition, the IC50 values can be calculated, and they are 113.7 μg/mL and 201.0 μg/mL for TC and NC when the HepG 2 cell was used, while they are 217.3 μg/mL and 174.9 μg/mL for TC and NC when the NIT3H3 cell was used.

Flow Cytometry. To further study the effect of targeting, we evaluate the differences of cytophagy between targeted TCs and NCs under different conditions by using flow cytometry. Figure 7a,d shows the result that TCs have higher selectivity to HepG2 cells, while both TCs and NCs exhibit the same in NIH3T3 cells, which are very similar to the result of cytotoxicity. When galactose inhibitors, galactosamines, were added to the HepG2 cells, Figure 7b shows the result that TCs even had less selectivity to the HepG2 cells owing to the inhibition of targeting group. It also illustrates that the galactose plays a critical role in the process of copolymers transporting into the cells. The inhibition of galactose might hinder the transportation, so it exhibited less selectivity. When the temperature was decreased to 4 °C, as shown in Figure 7c, these two copolymers exhibited the same selectivity due to the fact that the selectivity to galactose of ASGP-R on the surfaces of HepG2 cells reduced at low temperature.

Studies on Cellular Internalization. HepG2 and NIH3T3 cells were treated with the copolymer of equivalent doxorubicin concentration for 24 h. Alexa 488-phalloidin was used to label the cytoskeleton F-actin while DAPI was used to stain the cell

DOI: 10.1021/am508291k
ACS Appl. Mater. Interfaces 2015, 7, 2104−2115

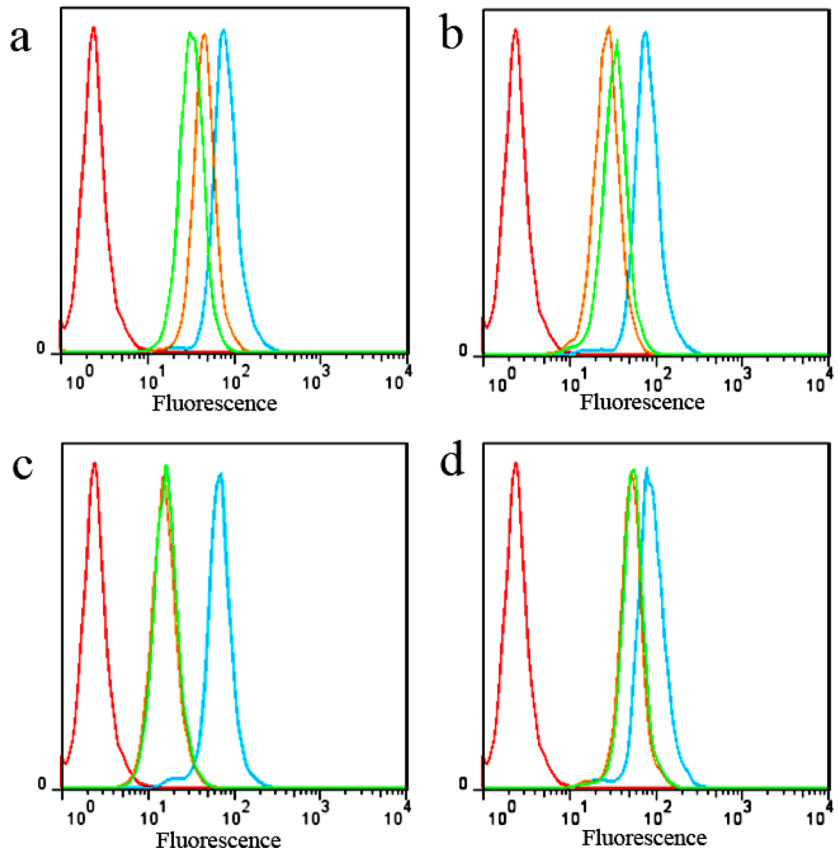

Figure 7. DOX-positive cell populations measured by flow cytometry of HepG2 cells cultured with TCs (orange), NCs (green), and free doxorubicin (blue), respectively, at (a) 37 °C and (c) 4 °C. (b) Galactosamines were added and the cells were cultured at 37 °C. (d) NIT3H3 cells were used instead and cultured at 37 °C.

nuclei. A confocal laser scanning microscope (CLSM) was used to observe the cells at various times (2 h, 6 h, 12 h, 24 h). Figure 8 shows the result of HepG2 and NIH3T3 cells cultured

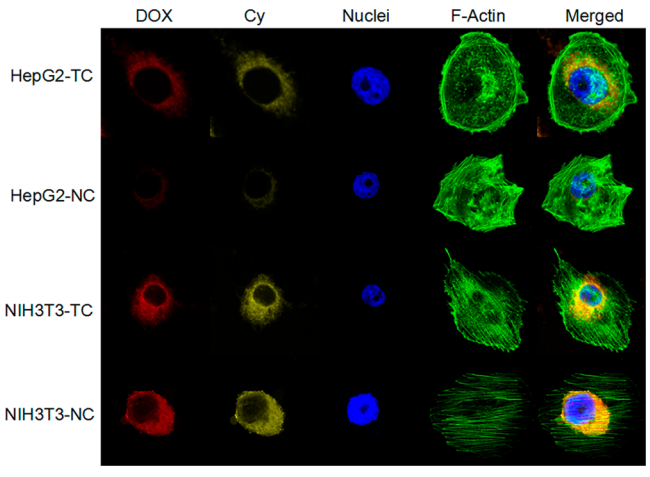

Figure 8. Image of LSM of HepG2 cells and NIH3T3 cells cultured with TCs and NCs, respectively, for 2 h.

with TCs and NCs for 2 h, respectively. Compared with images of NIH3T3 cells, HepG2 cells cultured with TCs and NCs exhibited significant differences in the intensity of fluorescence, indicating the different selectivity of gal targeted TCs and NCs to HepG2 and NIH3T3 cells as introduced above. The results of HepG2 cells cultured with TCs, NCs, and CWDs are shown in Figure 9. For CWDs (Figure 9c), the intensity of the cyanine dye increased as the time passed, which illustrated the aggregation of the copolymers in the cells as the time passed. The copolymers gathered around the cell nuclei but did not transport into it. For TCs (Figure 9a), little copolymers transported into the cells and dispersed in the cytoplasm after cultivation for 2 h. After 4 h, more copolymers gathered in the cytoplasm. Drug release did not happen due to the coincidence of the fluorescence of cyanine dye and doxorubicin. From the image of cultivation for 12 h, it could be obviously observed that the doxorubicin separated from the copolymer and transported into the cell nuclei, while the copolymers still retained in the cytoplasm which is similar to the result of CWDs. After 24 h, more drug release happened and the vast majority of the drug transported into the cell nuclei. By comparison, cells cultivated with NCs have weaker fluorescence intensity, which illustrated that less copolymers transported into the cells (Figure 9b). The drug release result is similar to that of TCs. Most of the doxorubicin entered into the cell nuclei after release from the copolymer. Small amount of doxorubicin and copolymers remained in the cytoplasm outside the nucleus.

CONCLUSION

A galactose targeting and pH-responsive triblock copolymer has been synthesized by a combination of ROP, RAFT polymerization, and click reaction. The copolymer micelles with strong emission in the near-infrared field have excellent biocompatibility and low toxicity in vitro. After conjugation of DOX and

DOI: 10.1021/am508291k
ACS Appl. Mater. Interfaces 2015, 7, 2104−2115

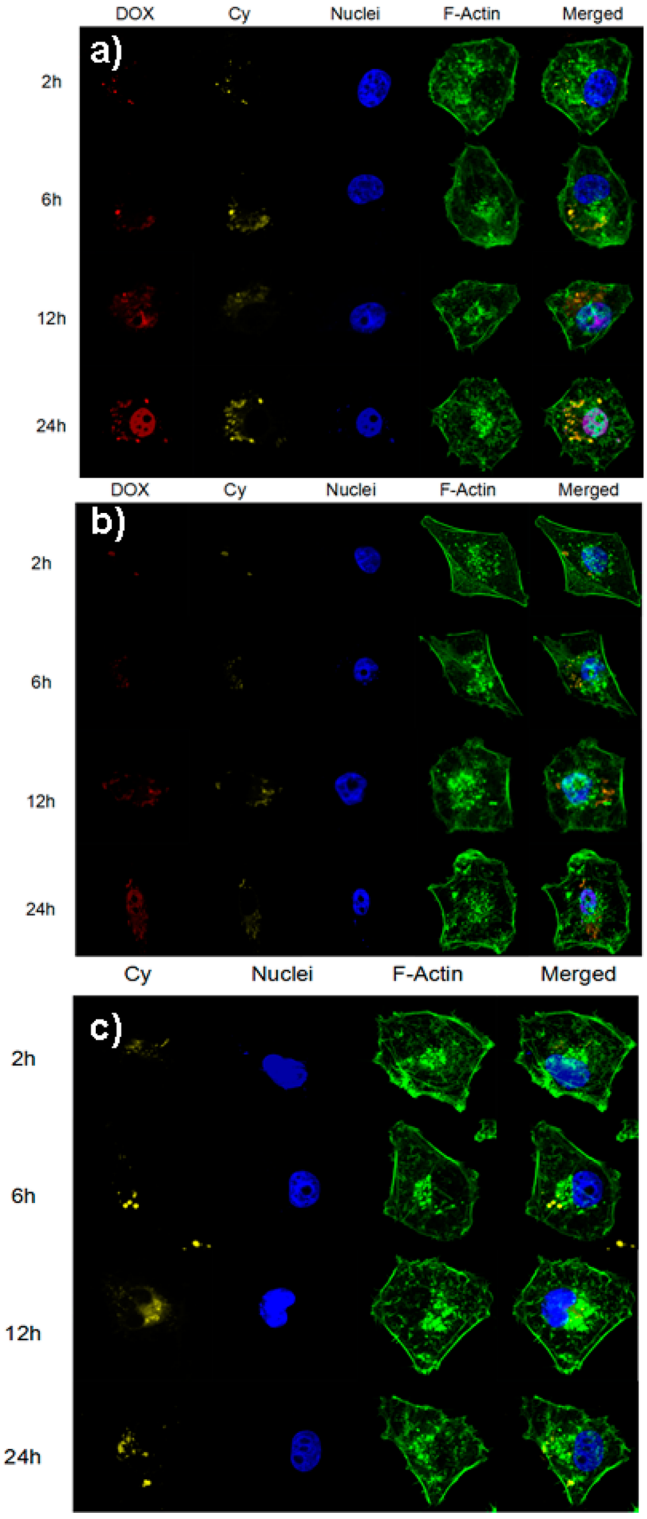

Figure 9. Images of LSM of HepG2 cells which were cultured with (a) TCs, (b) NCs, and (c) CWDs for 2 h, 6 h, 12 h, and 24 h, respectively.

NIR probe into the copolymer chain covalently, an intelligent theranostic target polymeric prodrug had been prepared. The prodrug show higher selectivity to the Hepatoma cells due to a ligand−receptor-recognition process compared to other cancer cells. The doxorubicin can be released from the copolymer as the pH changes from neutral to acidic, which could kill the targeting cancer cells in a short time. The polymeric prodrug is a potential theranostic agent for liver cancer treatment.

EXPERIMENTAL SECTION

Materials. Unless specifically indicated, the chemical reagents were purchased from Sinoreagent Corporation. Anhydrous tetrahydrofuran (THF) and *n*-hexane were produced by refluxing with CaH_2 overnight and then distilling. *N*,*N*-Dimethylformamide (DMF) was dried over CaH_2 at room temperature for 36 h followed by vacuum distillation. 4,4′-Azobis(4-cyanovaleric acid), 3-chloropropylamine hydrochloride, sodium azide, *N*,*N*′-dicyclohexyl carbodiimide (DCC), azodiisobutyronitrile (AIBN), *N*-hydroxysuccinimide (HOSu), methacryloyl chloride, epsilon-carbobenzoxy-L-lysine, triphosgene, *β*-benzyl-L-aspartate, doxorubicin hydrochloride, hydrazine dihydrochloride, propargylamine (PA amine), diisopropylethylamine (DIEA), *N*,*N*,*N*′,*N*′,*N*′-pentamethyldiethylene triamine (PMEDTA), 2,3,3-trimethylbenzoindolenine, 6-aminocaproic acid, and 3-bromopropionic acid were purchased from Aladdin Corporation, China. Oligo(ethylene glycol) methacrylate (OEGMA) was purchased from Sigma-Aldrich Corporation, China. Alexa Fluor 488-phalloidin and 4′6-diamidino-2-phenylindole (DAPI) were purchased from Invitrogen, Carlsbad. Milli-Q water (18.2 MΩ) was prepared using a Milli-Q Synthesis System (Millipore). Dialysis bags (cut off M_w = 2000 or 8000) were obtained from Bomei Biotechnology Corporation, China. The normal phase column chromatography process used the mixture of 100-200 and 200-300 mesh silica gel (Yantai Institute of Chemical Engineering, China).

Synthesis of *S*-Dodecyl-*S*′-(*α*-methyl-*α*-cyanobutyric acid) Trithiocarbonate (1). In total, 10.12 g (0.05 mol) of 1-dodecanethiol was dissolved into 40 mL of 10% ethanol aqueous solution in a round-bottom flask, then 3.37 g (0.06 mol, 1.2 equiv) of KOH was added. The obtained mixture was stirred for 0.5 h at room temperature, and then 3.0 mL (0.05 mol, 1 equiv) of CS_2 was added dropwise in 20 min. After stirred for 3 h, 10 mL of dichloromethane (DCM) containing 4.65 g (0.025 mol, 0.5 equiv) of 4-toluene sulfonyl chloride was dropped under an ice−water bath, and the mixture was further stirred for 5 h at room temperature. The organic layer was subsequently separated, and the aqueous solution was extracted with 10 mL of DCM three times. The organic phases were combined and washed with saturated sodium bicarbonate solution and sodium chloride solution three times, respectively. The obtained organic solution was dried with anhydrous magnesium sulfate. After filtering out the solid, the solvent was removed under vacuum yielding 11 g (79.4% yield) of deep red solid.

In total, 9.96 g (0.018 mol) of deep red intermediate was dissolved in 80 mL of acetic ether, and then 5.55 g (0.0198 mol, 1.1 equiv) of 4,4′-azobis(4-cyanovaleric acid) was added. The mixture was kept at 80 °C and stirred for 12 h. After removing the solvent under vacuum, the obtained red solid were purified by normal phase chromatography with a gradient elution from *n*-hexane to EtAc/*n*-hexane (4:1). Removing solvent after column chromatography yields 7.3 g (50.3% yield) of yellow solid. ^{1}H NMR (300 MHz, $CDCl_3$) δ 3.28 (t, J = 7.4 Hz, 2H), 2.53 (t, J = 7.4 Hz, 2H), 2.36 (t, J = 7.4 Hz, 2H), 1.77(s, 3H), 1.74−1.60 (m, 1H), 1.26 (18H), 0.88 (t, J = 6.2 Hz, 3H).

Synthesis of 3-Azidopropan-1-amine (APA). A total of 4 g (30.8 mmol) of 3-chloropropylamine hydrochloride and 6 g (92.3 mmol, 3 equiv) of sodium azide were reacted in 40 mL of water at 100 °C for 48 h. The reaction mixture was cooled to room temperature and extracted with 10 mL of DCM three times. The organic layer was separated, dried over $MgSO_4$, and filtered. Removing the solvent obtains 2.1 g (64.7% yield) of transparent liquid. ^{1}H NMR (300 MHz, $CDCl_3$) δ 3.38 (t, J = 6.7 Hz, 2H), 2.81 (t, J = 6.8 Hz, 2H), 1.74 (tt, J = 6.8 Hz, 6.7 Hz 2H).

Synthesis of APA-RAFT (2). In total, 750 mg (1.86 mmol) of RAFT agent 1 and 235 mg (2.05 mmol, 1.1 equiv) of HOSu were dissolved into 30 mL of dry DCM solution, followed by the addition dropwise of 5 mL of dry DCM solution containing 423 mg (2.05 mmol, 1.1 equiv) of DCC in an ice-water bath. The obtained mixture was stirred for 36 h. After the solid was removed by filtration, 187 mg (1.86 mmol, 1 equiv) of APA was added. After stirring for another 12 h at room temperature, the solvent was removed under vacuum. The raw product was further purified by normal phase chromatography

DOI: 10.1021/am508291k
ACS Appl. Mater. Interfaces 2015, 7, 2104−2115

with a gradient elution from petroleum ether to EtAc/petroleum ether (3.5:6.5). After the solvent was removed, 560 mg (62% yield) of yellow solid was obtained. ^{1}H NMR (300 MHz, $CDCl_3$) δ 3.41−3.33 (m, 2H), 3.31−3.23 (m, 2H), 2.32 (s, 4H), 1.84−1.77 (m, 4H), 1.75 (s, 3H), 1.70−1.62 (m, 2H), 0.87 (t, J = 6.2 Hz, 3H). IR (thin film, cm^{-1}) 1659, 2097, 2851, 2922, 3439.

Synthesis of Polymer 3 (APA-RAFT-POEGMA). To a Schlenk tube, 230 mg (0.474 mmol) of RAFT-APA and 54 mg of AIBN was dissolved in 1 mL of DMF, 250 μL of the the mixture was added to the solution (0.085 mmol, 0.2 equiv), and 6.8 g (14.2 mmol, 30 equiv) of OEGMA was dissolved in 5 mL of DMF under the protection of argon gas. The mixture was kept at 80 °C under stirring for 12 h. Then the obtained solution was purified by dialysis against ultrapure water. In total, 5.4 g (98.8% yields) of yellow solid was obtained after removing water by freeze-drying.

Synthesis of 1,2:3,4-Di-*O*-isopropylidene-D-galactopyranose(pGP). In total, 15.0 g (110.1 mmol) of anhydrous $ZnCl_2$ was added into 130 mL of dry acetone under stirring with nitrogen, and 0.9 mL of concentrated H_2SO_4 and 12 g (66.7 mmol) of D-galactose was added and stirred for 5 h at room temperature. Then a suspension of 24 g of Na_2CO_4 in 42 mL of water was added. After removing the precipitate, the filtrate was subjected to rotary evaporation to remove the added acetone. Then the aqueous phase was extracted with 40 mL of diethyl ether three times, and the ether solution was dried over anhydrous magnesium sulfate followed by rotary evaporation, and 12 g (69.2% yield) of product was obtained as a white solid.

Synthesis of 6-*O*-Methacryloyl-1,2:3,4-di-*O*-isopropylidene-D-galactopyranose (MAlpGP). A volume of 22.15 mL (0.22 mol, 5 equiv) of methacryloyl chloride was added dropwise to a stirred suspension of 11.39 g (0.044 mol) of pGP and 9.33 g (0.092 mol, 2.1 equiv) of basic alumina in 135 mL of distilled acetonitrile in an ice-water bath. The mixture was stirred at room temperature for 3 days. After removing solids, solvent was removed under vacuum and a light yellow oil was obtained, which was further purified via column chromatography (hexane/ethyl acetate, 8:1 v/v). Removing solvent yields 8.4 g (58.2% yield) of white solid.

Synthesis of Polymer 4 (APA-RAFT-PMalpGP-*b*-POEGMA). To a flame argon purged Schlenk tube, 400 mg (34.7 μmol) of **3** and 40 mg of AIBN was dissolved in 1 mL of DMF, 30 μL of the mixture was added to the solution (7 μmol, 0.2 equiv), and 114 mg (0.347 mmol, 10 equiv) of MAlpGP was dissolved in 5 mL of DMF under argon. The mixture was kept at 80 °C and stirred for 24 h. The obtained solution was purified by dialysis and 475 mg (99% yield) of product as pale yellow solid was obtained by freeze-drying.

Synthesis of Llys-NCA. In total, 3.0 g (10.7 mmol) of nepsilon-carbobenzoxy-L-lysine was suspended, and 3.19 g (10.7 mmol 1 equiv) of triphosgene was dissolved in dry THF (40 mL). The obtained suspension was stirred at 45 °C for 2 h, traces of unreacted nepsilon-carbobenzoxy-L-lysine were removed by filtration, and the filtrate was crystallized two times by a mixture of THF and hexane to form 2.27 g (69.3% yield) of anhydride as yellow crystals.

Synthesis of Asp-NCA. The synthesis is the same as the method of Llys-NCA. In brief, 3 g (13.4 mmol) of L-aspartic acid-4-benzyl ester and 4 g (13.4 mmol 1 equiv) of triphosgene was stirred in 40 mL of dry DMF at 45 °C for 2 h. A total of 2.7 g (68% yield) of white solid was collected after purification.

Synthesis of Polymer 5 (PA-P(Llys-*co*-Asp)). To a flame-dried Schlenk tube purged with argon, 21.6 mg (0.392 mmol) of propargylamine was added, then 5 mL of dry DMF was added to solubilize the initiator. The mixture was then precooled in an ice-water bath. A total of 1.2 g (3.92 mmol, 10 equiv) of Llys-NCA was dissolved in 5 mL of DMF, and 937 mg (3.92 mmol, 10 equiv) of Asp-NCA in 5 mL of DMF solution were added to the initiator solution successively. The mixture was stirred at 0 °C for 3 days, after which 94 mg (0.431 mmol, 1.1 equiv) of Boc_2O was added and the solution was stirred at room temperature for another 12 h. Then the solution was precipitated using 100 mL of cold ether, and the obtained white solid was redissolved in 5 mL of DMF and further purified by dialysis. Removing water by freeze-drying gives 1.63 g (95.4% yield) of product as a white solid.

Synthesis of Triblock Copolymer 6 by Using Click Reaction. To a flame-dried Schlenk tube purged with argon, 5 mg (34.7 μmol, 1 equiv) of CuBr was added to 3 mL of DMF solution containing 480 mg (34.7 μmol) of polymer **4**, 151.2 mg (34.7 μmol, 1 equiv) of polymer **5**, and 6 mg (34.7 μmol, 1 equiv) of PMEDTA. The reaction mixture was stirred at 30 °C for 3 days and quenched by exposure to air. The solution was purified by extensive dialysis against EDTA aqueous solution for 12 h and water for another 12 h. Removing water by freeze-drying forms 578 mg (91.6% yield) of product as a white solid.

Deprotection of pGP of Copolymer 6. A total of 500 mg (27.5 μmol) of triblock copolymer **6** was stirred in 5 mL of 80% formic acid for 48 h at room temperature. Next, 3 mL of deionized water was added, and the solution was stirred for another 3 h. To remove formic acid, the solution was dialyzed against ultrapure water. In total, 410 mg (85.1% yield) of product as a yellow solid was obtained after removing water by freeze-drying.

Synthesis of Triblock Copolymer 7. In total, 350 mg (20 μmol) of the above product was dispersed into 5 mL of dry DMF, then addition of 90 mg (857 μmol, 42.5 equiv) of hydrazine dichloride and 0.284 mL (1.72 mmol, 85.9 equiv) of DIEA. The mixture was stirred at 45 °C for 36 h. After the solution is transparent, the mixture was dialyzed against water. Removal of water was performed by freeze-drying to get 315 mg (93.6% yields) of copolymer **7** as a yellow solid.

Addition of Drug. A total of 285 mg (16.9 μmol) of copolymer **7** was dissolved in 5 mL of DMF, and 19.4 mg (33.4 μmol, 1.98 equiv) of doxorubicin hydrochloride was added. The as-formed red solution was stirred at 45 °C in the dark for 48 h. Then the mixture was further purified by dialysis. In total, 267 mg (90.1% yield) of product as a red powder was obtained after removal of water by freeze-drying.

Synthesis of 1-Hydroxycarbonylethyl-2,3,3-trimethylbenzoindoleninium Bromide (9). In total, 2.0 g (9.56 mmmol) of 2,3,3-trimethylbenzo-indolenine was dissolved in 30 mL of 1,2-dichlorobenzene, then addition of 1.45 g (9.56 mmol, 1 equiv) of 3-bromopropionic acid, and the mixture was refluxed at 110 °C for 10 h. On cooling the solution to room temperature, the product was separated from the solution as rose red solids. Then a mixture of ether and chloroform was used to wash the product, and 2.9 g (84% yield) of rosy red powder was obtained after it was dried under vacuum.

Synthesis of 2-Chloro-1-formyl-3-(hydroxymethylene)-cyclohex-1-ene (10). In an ice-water bath, 34 mL (442 mmol, 5 equiv) of DMF was mixed with 40 mL of DCM. A volume of 32 mL (343 mmol, 4 equiv) of $POCl_3$ dissolved in 30 mL of DCM was slowly added via a constant pressure drop funnel. Then, 8.53 g (84.6 mmol) of cyclohexanone was hereby added dropwise. The as-obtained mixture was refluxed for 2 h, and then the oil-like red residue was poured into 100 mL of ice. The mixture was stored at 4 °C overnight for the formation of crystals. After filtration, a yellow crystal was obtained, and then it was recrystallized from a mixture of acetone and DCM to form the 6.4 g (44% yield) of product as a yellow solid.

Synthesis of Parent Cyanine Dye (11). In total, 1.0 g (2.77 mmol) of salt **9** and 238 mg (1.39 mmol, 0.5 equiv) of product **10** were dispersed into a mixture solvent of 35 mL of *n*-butanol and 15 mL of benzene in a two neck flask fitted with a Dean−Stark trap and a condenser (see Scheme 3). The solution was stirred for 16 h at 110 °C under a nitrogen atmosphere, and then the solvent was removed under vacuum. Next, the obtained solid was purified using normal phase column chromatography with a gradient elution from EtOAc to EtOAc/methanol (4:1). Removing solvent yields 0.93 g (86.3% yield) of deep green solid.

Synthesis of Aminocyanine Dye (12). In total, 400 mg (0.514 mmol) of cyanine dye **11** and 67.4 mg (0.514 mmol, 1 equiv) of 6-aminocaproic acid was added to 5 mL of dry DMF, with the addition of 87 μL (0.514 mmol, 1 equiv) of DIEA (see Scheme 3). The obtained solution was stirred at 70 °C in the dark for 8 h. After removing the solvent under vacuum, the obtained deep blue solid was further purified by a column chromatography method with gradient

DOI: 10.1021/am508291k
ACS Appl. Mater. Interfaces 2015, 7, 2104−2115

Scheme 3. Synthesis of the Near Infrared Aminocyanine Dye

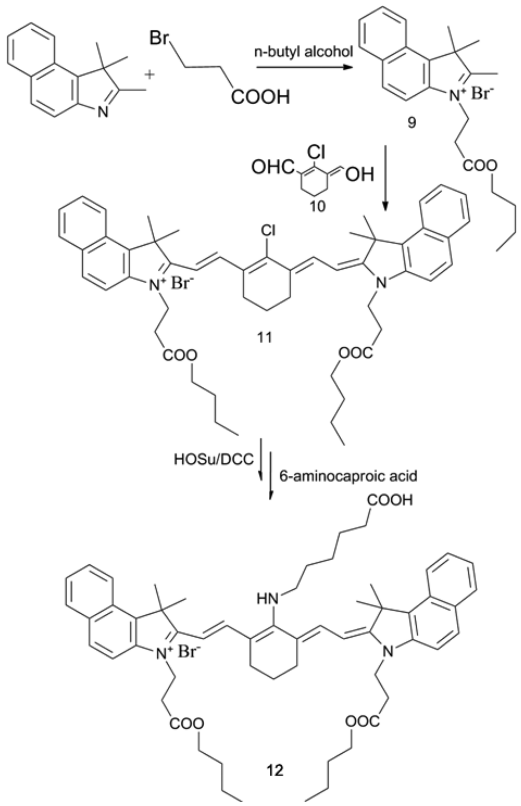

elution from EtOAc to EtOAc/methanol (4:1). Removing solvent yields 274 mg (61.1% yield) of deep blue solid.

Addition of Cyaminocyanine Dye to Copolymer 8. In total, 5 mg (5.73 μmol) of aminocyanine dye **12** was dispersed into 0.8 mL of dry DMF, with the addition of 0.2 mL of DMF containing 0.8 mg (6.95 μmol, 1.21 equiv) of HOSu and 1.4 mg (6.79 μmol, 1.18 equiv) of DCC. The mixture was stirred for 24 h at room temperature in the dark. Samples of 100 μL volume were removed from the mixture by a pipet and added to a DMF solution containing 100 mg (5.7 μmol) of copolymer **7**. The mixture was stirred for 24 h at room temperature in the dark. The obtained solution was dialyzed against deionized water. A mass of 89 mg (88.6% yields) of final product as a blue solid was obtained after removing the water by freeze-drying.

Synthesis of Nontargeting Copolymers (NC) and Copolymers without Drugs (CWDs). The synthesis of NC and CWD was similar to that of TC. The structure of NC is POEGMA-*b*-P(Llys-*co*-Asp-DOX)-Cy without the polymerization of MalpGP compared to TC. On the other hand, the structure of CWD is PMalGP-*b*-POEGMA-*b*-P(Llys-*co*-Asp)-Cy without the conjugation of doxorubicin. The method of synthesis was like the steps given above.

The drug concentration was determined using UV spectrophotometer at the wavelength of 480 nm. The content of drug conjugation (the ratio of drug weight to prodrug weight) was 4.0% for TC and 6.5% for NC.

Preparation of Micelles. In total, 5 mg of TC (NC or CWD) was dissolved in 1 mL of DMF. Then the solution was sealed in a dialysis bag and was dialyzed for 1 day against water.

Characterization. ^{1}H NMR and ^{13}C NMR spectra were measured using a Bruker AC 300 spectrometer. Deuterated dimethyl sulfoxide (DMSO) and deuterated chloroform containing 0.03 vol % tetramethylsilane (TMS) were used as the solvent. Fluorescence spectrophotometer (Shimadzu RF-5301PC) was used to measure the florescence behavior of the samples with excitation and emission slit widths of 10 and 10 nm, respectively. UV−vis spectra were obtained on a Shimadzu UV-2401 PC Ultraviolet. A Bruker EQUINOX 55 Fourier transform-infrared spectrometer was used to measure the FT-IR spectra by the KBr disk method. Molecular weights of the samples were determined by gel permeation chromatography (GPC, LC-20AD, Shimadzu) equipped with one Shodex GPC KD-804 column, a refractive index detector (RID-10A), and a spectrofluorometric detector (RF-20Axs, Shimadzu). DMF was used as the mobile phase while the concentration of the sample is 5 mg/mL and the measurement was performed at 60 °C. Monodispersed standard polystyrene samples were used for the calibration of M_n, M_w, and M_w/M_n. Field emission transmission electron microscopy measurements were performed on a JEM-2100F microscope. Size and size distribution of the micelle solution was measured by dynamic light scattering (DLS) using a Malvern Zetasizer Nano ZS90 with a He−Ne laser (633 nm) and 90° collecting optics. The solution was measured at room temperature, and the results were analyzed by the Malvern Dispersion Technology Software 4.20. The absorbance for cytotoxicity was measured by using a Biorad 680 microplate reader. The results of the flow cytometry were collected on a FACSCalibur flow cytometer (BD Biosciences) and then analyzed with WinMDI 2.9 software. The laser scanning confocal microscope measurements was carried out on LSM 710 Meta (Carl Zeiss Inc., Thornwood, NY).

In Vitro Drug Release. Drug release behavior of the copolymers was measured under both neutral and acidic microenvirongments. For the neutral condition, 200 μL (10 mg/mL) of copolymer solution (1 mg/mL) was sealed in a dialysis bag, followed by being immersed in 50 mL of 0.2 M phosphate buffered saline (PBS) solution. This measurement was evaluated at 37 °C on a shaking bath. At a predetermined time points, 2 mL of sample was removed with 2 mL of fresh PBS added at the same time. Quantified testing was performed by calculating the intensity of the emission wavelength at 577 nm, with an excitation wavelength of 480 nm by utilizing the fluorospectrophotometer. For acidic conditions, the method is similar but employing 0.2 M acetate buffer as the release media instead.

Cytotoxicity. The cytotoxicity of the copolymers was performed with a methyl tetrazolium (MTT) viability assay against both the NIT3H3 and HepG2 cells. Typically, HepG2 cells were seeded in 100 μL of DMEM in 96-well plates at a density of 5000 cells per well and incubated for 24 h. Followed by the replacement of DMEM containing free DOX or the three different copolymers, we synthesized at various concentrations. After incubation for 72 h, the medium was replaced by 100 μL of fresh DMEM, followed by the addition of 25 μL of MTT solution (5 mg/mL in PBS) to each well. Then the cells were cultivated at 37 °C for 2 h with the addition of 100 μL of 20% sodium dodecyl sulfate in 50% DMF solution for the next step, and then the plate was incubated for another 4 h at 37 °C. The absorbance of the wells was measured at 480 nm. By normalizing the cell viability to that of control cells cultivated in the medium without the drug, the cytotoxicity was further analyzed. The measurement of the copolymer cytotoxicity for NIT3H3 cells was carried out in a similar way.

Flow Cytometry. HepG2 cells were cultured in 0.5 mL of DMEM in 24-well plates at a density of 5×10^4 cells per well. The cells were cultivated overnight, followed by the replacement of the medium with DMEM containing 4 μg/mL free doxorubicin or copolymers with an equivalent concentration of DOX. After incubating the cells at 37 or 4 °C for 2 h, while some other cells were incubated with excessive galactosamine, the cells were washed with cold PBS (pH = 7.4) twice. The resulting cells were resuspended in 200 μL of PBS for FACS analyses. NIT3H3 cells were measured in a similar way just at 37 °C.

Cellular Uptake Study. HepG2 cells were seeded on 14 mm coverslips in 1.0 mL of DMEM in 12-well plates at a density of 3×10^4 cells per well and cultured at 37 °C overnight. After incubating the cells in DMEM with copolymers at an equivalent doxorubicin concentration of 4 μg/mL for 2 h, the culture medium was discarded, followed by washing the cells with cold PBS twice. Then the cells were incubated for 2 h, 6 h, 12 h, and 24 h and fixed with 4% paraformaldehyde at room temperature for 15 min. The skeleton of the cells was further stained with Alexa Fluor 488-phalloidin according to the supplied protocol, while the cell nuclei were labeled with 4′,6-diamidino-2-phenylindole. After dropping antifade mounting medium on glass microscope slides, which were mounted on by the overslips, images of the cells were captured by a laser scanning confocal microscope.

DOI: 10.1021/am508291k
ACS Appl. Mater. Interfaces 2015, 7, 2104−2115

■ ASSOCIATED CONTENT

Supporting Information

NMR and FT-IR spectra of the intermediates and table of their molecular weights. This material is available free of charge via the Internet at http://pubs.acs.org.

■ AUTHOR INFORMATION

Corresponding Author

*E-mail: lfyan@ustc.edu.cn. Fax: +86-551-63603748. Phone: +86-551-63606853.

Notes

The authors declare no competing financial interest.

■ ACKNOWLEDGMENTS

This work is supported by the National Basic Research Program of China (Grant No. 2011CB921403) and the National Natural Science Foundation of China (Grant No. 51373162).

■ REFERENCES

(1) Zhang, Z. J.; Wang, J.; Nie, X.; Wen, T.; Ji, Y. L.; Wu, X. C.; Zhao, Y. L.; Chen, C. Y. Near Infrared Laser-Induced Targeted Cancer Therapy Using Thermoresponsive Polymer Encapsulated Gold Nanorods. *J. Am. Chem. Soc.* **2014**, *136*, 7317−7326.

(2) Joglekar, M.; Trewyn, B. G. Polymer-Based Stimuli-Responsive Nanosystems for Biomedical Applications. *Biotechnol. J.* **2013**, *8*, 931−U78.

(3) Shim, M. S.; Kwon, Y. J. Stimuli-Responsive Polymers and Nanomaterials for Gene Delivery and Imaging Applications. *Adv. Drug Delivery Rev.* **2012**, *64*, 1046−1058.

(4) Ge, Z. S.; Liu, S. Y. Functional Block Copolymer Assemblies Responsive to Tumor and Intracellular Microenvironments for Site-Specific Drug Delivery and Enhanced Imaging Performance. *Chem. Soc. Rev.* **2013**, *42*, 7289−7325.

(5) Guo, Z. Q.; Park, S.; Yoon, J.; Shin, I. Recent Progress in the Development of near-Infrared Fluorescent Probes for Bioimaging Applications. *Chem. Soc. Rev.* **2014**, *43*, 16−29.

(6) Biju, V. Chemical Modifications and Bioconjugate Reactions of Nanomaterials for Sensing, Imaging, Drug Delivery and Therapy. *Chem. Soc. Rev.* **2014**, *43*, 744−764.

(7) Yen, S. K.; Janczewski, D.; Lakshmi, J. L.; Bin Dolmanan, S.; Tripathy, S.; Ho, V. H. B.; Vijayaragavan, V.; Hariharan, A.; Padmanabhan, P.; Bhakoo, K. K.; Sudhaharan, T.; Ahmed, S.; Zhang, Y.; Selvan, S. T. Design and Synthesis of Polymer-Functionalized Nir Fluorescent Dyes-Magnetic Nanoparticles for Bioimaging. *ACS Nano* **2013**, *7*, 6796−6805.

(8) Basuki, J. S.; Duong, H. T. T.; Macmillan, A.; Erlich, R. B.; Esser, L.; Akerfeldt, M. C.; Whan, R. M.; Kavallaris, M.; Boyer, C.; Davis, T. P. Using Fluorescence Lifetime Imaging Microscopy to Monitor Theranostic Nanoparticle Uptake and Intracellular Doxorubicin Release. *ACS Nano* **2013**, *7*, 10175−10189.

(9) Muthu, M. S.; Leong, D. T.; Mei, L.; Feng, S. S. Nanotheranostics - Application and Further Development of Nanomedicine Strategies for Advanced Theranostics. *Theranostics* **2014**, *4*, 660−677.

(10) Svenson, S. Theranostics: Are We There Yet? *Mol. Pharmaceutics* **2013**, *10*, 848−856.

(11) Feng, L.; Liu, L.; Lv, F.; Bazan, G. C.; Wang, S. Preparation and Biofunctionalization of Multicolor Conjugated Polymer Nanoparticles for Imaging and Detection of Tumor Cells. *Adv. Mater.* **2014**, *26*, 3926−3930.

(12) Yin, M.; Shen, J.; Pflugfelder, G. O.; Müllen, K. A Fluorescent Core−Shell Dendritic Macromolecule Specifically Stains the Extracellular Matrix. *J. Am. Chem. Soc.* **2008**, *130*, 7806−7807.

(13) Louie, A. Y. Multimodality Imaging Probes: Design and Challenges. *Chem. Rev.* **2010**, *110*, 3146−3195.

(14) Laurent, S.; Forge, D.; Port, M.; Roch, A.; Robic, C.; Elst, L. V.; Muller, R. N. Magnetic Iron Oxide Nanoparticles: Synthesis, Stabilization, Vectorization, Physicochemical Characterizations, and Biological Applications. *Chem. Rev.* **2008**, *108*, 2064−2110.

(15) Mornet, S.; Vasseur, S.; Grasset, F.; Duguet, E. Magnetic Nanoparticle Design for Medical Diagnosis and Therapy. *J. Mater. Chem.* **2004**, *14*, 2161−2175.

(16) Michalet, X.; Pinaud, F. F.; Bentolila, L. A.; Tsay, J. M.; Doose, S.; Li, J. J.; Sundaresan, G.; Wu, A. M.; Gambhir, S. S.; Weiss, S. Quantum Dots for Live Cells, in Vivo Imaging, and Diagnostics. *Science* **2005**, *307*, 538−544.

(17) Gao, X. H.; Cui, Y. Y.; Levenson, R. M.; Chung, L. W. K.; Nie, S. M. In Vivo Cancer Targeting and Imaging with Semiconductor Quantum Dots. *Nat. Biotechnol.* **2004**, *22*, 969−976.

(18) Medintz, I. L.; Uyeda, H. T.; Goldman, E. R.; Mattoussi, H. Quantum Dot Bioconjugates for Imaging, Labelling and Sensing. *Nat. Mater.* **2005**, *4*, 435−446.

(19) He, X.; Gao, J.; Gambhir, S. S.; Cheng, Z. Near-Infrared Fluorescent Nanoprobes for Cancer Molecular Imaging: Status and Challenges. *Trends Mol. Med.* **2010**, *16*, 574−583.

(20) Frangioni, J. V. In Vivo near-Infrared Fluorescence Imaging. *Curr. Opin. Chem. Biol.* **2003**, *7*, 626−634.

(21) Weissleder, R.; Tung, C. H.; Mahmood, U.; Bogdanov, A. In Vivo Imaging of Tumors with Protease-Activated near-Infrared Fluorescent Probes. *Nat. Biotechnol.* **1999**, *17*, 375−378.

(22) Barth, B. M.; Altinoglu, E. I.; Shanmugavelandy, S. S.; Kaiser, J. M.; Crespo-Gonzalez, D.; DiVittore, N. A.; McGovern, C.; Goff, T. M.; Keasey, N. R.; Adair, J. H.; Loughran, T. P., Jr.; Claxton, D. F.; Kester, M. Targeted Indocyanine-Green-Loaded Calcium Phosphosilicate Nanoparticles for in Vivo Photodynamic Therapy of Leukemia. *ACS Nano* **2011**, *5*, 5325−5337.

(23) Chi, X.; Huang, D.; Zhao, Z.; Zhou, Z.; Yin, Z.; Gao, J. Nanoprobes for in Vitro Diagnostics of Cancer and Infectious Diseases. *Biomaterials* **2012**, *33*, 189−206.

(24) Liu, L. X.; Xing, T.; Mao, C. Q.; Lai, B.; Yan, L. F. Preparation of near-Infrared Pegylated Polypeptide for Potential Visible Drug Delivery. *J. Macromol. Sci. Part a-Pure Appli. Chem.* **2013**, *50*, 90−98.

(25) Xing, T.; Lai, B.; Mao, C. Q.; Yan, L. F. Synthesis of Nir Probe Conjugated Polypeptide for Drug Delivery and Imaging. *J. Controlled Release* **2013**, *172*, E50−E50.

(26) Xing, T.; Lai, B.; Yan, L. F. Disulfide Cross-Linked Polypeptide Nanogel Conjugated with a Fluorescent Probe as a Potential Image-Guided Drug-Delivery Agent. *Macromol. Chem. Phys.* **2013**, *214*, 578−588.

(27) Xing, T.; Yan, L. F. Ph-Responsive Amphiphilic Block Copolymer Prodrug Conjugated near Infrared Fluorescence Probe. *RSC Adv.* **2014**, *4*, 28186−28194.

(28) Xing, T.; Yang, X. Z.; Wang, F.; Lai, B.; Yan, L. F. Synthesis of Polypeptide Conjugated with near Infrared Fluorescence Probe and Doxorubicin for Ph-Responsive and Image-Guided Drug Delivery. *J. Mater. Chem.* **2012**, *22*, 22290−22300.

(29) Li, J.; Guo, K.; Shen, J.; Yang, W.; Yin, M. A Difunctional Squarylium Indocyanine Dye Distinguishes Dead Cells through Diverse Staining of the Cell Nuclei/Membranes. *Small* **2014**, *10*, 1351−1360.

(30) Alarcon, C. D. H.; Pennadam, S.; Alexander, C. Stimuli Responsive Polymers for Biomedical Applications. *Chem. Soc. Rev.* **2005**, *34*, 276−285.

(31) Schmaljohann, D. Thermo- and Ph-Responsive Polymers in Drug Delivery. *Adv. Drug Delivery Rev.* **2006**, *58*, 1655−1670.

(32) Ganta, S.; Devalapally, H.; Shahiwala, A.; Amiji, M. A Review of Stimuli-Responsive Nanocarriers for Drug and Gene Delivery. *J. Controlled Release* **2008**, *126*, 187−204.

(33) Kost, J.; Langer, R. Responsive Polymeric Delivery Systems. *Adv. Drug Delivery Rev.* **2001**, *46*, 125−148.

(34) Paramonov, S. E.; Bachelder, E. M.; Beaudette, T. T.; Standley, S. M.; Lee, C. C.; Dashe, J.; Frechet, J. M. J. Fully Acid-Degradable Biocompatible Polyacetal Microparticles for Drug Delivery. *Bioconj. Chem.* **2008**, *19*, 911−919.

DOI: 10.1021/am508291k
ACS Appl. Mater. Interfaces 2015, 7, 2104−2115

(35) Sun, A.; Li, Z.; Wei, T.; Li, Y.; Cui, P. Highly Sensitive Humidity Sensor at Low Humidity Based on the Quaternized Polypyrrole Composite Film. *Sensors Actuators B: Chem.* **2009**, *142*, 197−203.
(36) Zhou, L.; Cheng, R.; Tao, H.; Ma, S.; Guo, W.; Meng, F.; Liu, H.; Liu, Z.; Zhong, Z. Endosomal Ph-Activatable Poly(Ethylene Oxide)-Graft-Doxorubicin Prodrugs: Synthesis, Drug Release, and Biodistribution in Tumor-Bearing Mice. *Biomacromolecules* **2011**, *12*, 1460−1467.
(37) Bae, Y.; Fukushima, S.; Harada, A.; Kataoka, K. Design of Environment-Sensitive Supramolecular Assemblies for Intracellular Drug Delivery: Polymeric Micelles That Are Responsive to Intracellular Ph Change. *Angew. Chem., Int. Ed.* **2003**, *42*, 4640−4643.
(38) Ping, J. F.; Wang, Y. X.; Fan, K.; Wu, J.; Ying, Y. B. Direct Electrochemical Reduction of Graphene Oxide on Ionic Liquid Doped Screen-Printed Electrode and Its Electrochemical Biosensing Application. *Biosens. Bioelectron.* **2011**, *28*, 204−209.
(39) Meng, F.; Hennink, W. E.; Zhong, Z. Reduction-Sensitive Polymers and Bioconjugates for Biomedical Applications. *Biomaterials* **2009**, *30*, 2180−2198.
(40) Cerritelli, S.; Velluto, D.; Hubbell, J. A. Peg-Ss-Pps: Reduction-Sensitive Disulfide Block Copolymer Vesicles for Intracellular Drug Delivery. *Biomacromolecules* **2007**, *8*, 1966−1972.
(41) Gao, W.; Chan, J. M.; Farokhzad, O. C. Ph-Responsive Nanoparticles for Drug Delivery. *Mol. Pharmaceutics* **2010**, *7*, 1913−1920.
(42) Pan, D.; she, W.; Guo, C.; Luo, K.; Yi, Q.; Gu, Z. Pegylated Dendritic Diaminocyclohexyl-Platinum (Ii) Conjugates As ph-Responsive Drug Delivery Vehicles with Enhanced Tumor Accumulation and Antitumor Efficacy. *Biomaterials* **2014**, *35*, 10080−10092.
(43) Kataoka, K.; Matsumoto, T.; Yokoyama, M.; Okano, T.; Sakurai, Y.; Fukushima, S.; Okamoto, K.; Kwon, G. S. Doxorubicin-Loaded Poly(Ethylene Glycol)-Poly(Beta-Benzyl-L-Aspartate) Copolymer Micelles: Their Pharmaceutical Characteristics and Biological Significance. *J. Controlled Release* **2000**, *64*, 143−153.
(44) Janib, S. M.; Moses, A. S.; MacKay, J. A. Imaging and Drug Delivery Using Theranostic Nanoparticles. *Adv. Drug Delivery Rev.* **2010**, *62*, 1052−1063.
(45) Koo, H.; Huh, M. S.; Sun, I. C.; Yuk, S. H.; Choi, K.; Kim, K.; Kwon, I. C. In Vivo Targeted Delivery of Nanoparticles for Theranosis. *Acc. Chem. Res.* **2011**, *44*, 1018−1028.
(46) Caldorera-Moore, M. E.; Liechty, W. B.; Peppas, N. A. Responsive Theranostic Systems: Integration of Diagnostic Imaging Agents and Responsive Controlled Release Drug Delivery Carriers. *Acc. Chem. Res.* **2011**, *44*, 1061−1070.
(47) Koo, H.; Huh, M. S.; Sun, I.-C.; Yuk, S. H.; Choi, K.; Kim, K.; Kwon, I. C. In Vivo Targeted Delivery of Nanoparticles for Theranosis. *Acc. Chem. Res.* **2011**, *44*, 1018−1028.
(48) Brannon-Peppas, L.; Blanchette, J. O. Nanoparticle and Targeted Systems for Cancer Therapy. *Adv. Drug Delivery Rev.* **2004**, *56*, 1649−1659.
(49) Farokhzad, O. C.; Cheng, J. J.; Teply, B. A.; Sherifi, I.; Jon, S.; Kantoff, P. W.; Richie, J. P.; Langer, R. Targeted Nanoparticle-Aptamer Bioconjugates for Cancer Chemotherapy in Vivo. *Proc. Natl. Acad. Sci. U. S. A.* **2006**, *103*, 6315−6320.
(50) Liu, Y.; Li, K.; Pan, J.; Liu, B.; Feng, S.-S. Folic Acid Conjugated Nanoparticles of Mixed Lipid Monolayer Shell and Biodegradable Polymer Core for Targeted Delivery of Docetaxel. *Biomaterials* **2010**, *31*, 330−338.
(51) Sulistio, A.; Lowenthal, J.; Blencowe, A.; Bongiovanni, M. N.; Ong, L.; Gras, S. L.; Zhang, X.; Qiao, G. G. Folic Acid Conjugated Amino Acid-Based Star Polymers for Active Targeting of Cancer Cells. *Biomacromolecules* **2011**, *12*, 3469−3477.
(52) Yu, M.; Yutao, L.; Si-Shen, F. Formulation of Docetaxel by Folic Acid-Conjugated D-Alpha-Tocopheryl Polyethylene Glycol Succinate 2000 (Vitamin E Tpgs 2k) Micelles for Targeted and Synergistic Chemotherapy. *Biomaterials* **2011**, *32*, 4058−66.
(53) Hu, C.-M. J.; Kaushal, S.; Cao, H. S. T.; Aryal, S.; Sartor, M.; Esener, S.; Bouvet, M.; Zhang, L. Half-Antibody Functionalized Lipid-Polymer Hybrid Nanoparticles for Targeted Drug Delivery to Carcinoembryonic Antigen Presenting Pancreatic Cancer Cells. *Mol. Pharmaceutics* **2010**, *7*, 914−920.
(54) Omelyanenko, V.; Kopeckova, P.; Gentry, C.; Shiah, J. G.; Kopecek, J. Hpma Copolymer-Anticancer Drug-Ov-Tl-Tl16 Antibody Conjugates. 1. Influence of the Method of Synthesis on the Biding Affinity to Ovcar-3 Ovarian Carcinoma Cells in Vitro. *J. Drug Target.* **2003**, *11*, 295−309.
(55) Su, W.; Wang, H.; Wang, S.; Liao, Z.; Kang, S.; Peng, Y.; Han, L.; Chang, J. Peg/Rgd-Modified Magnetic Polymeric Liposomes for Controlled Drug Release and Tumor Cell Targeting. *Int. J. Pharm.* **2012**, *426*, 170−181.
(56) Temming, K.; Schiffelers, R. M.; Molema, G.; Kok, R. J. Rgd-Based Strategies for Selective Delivery of Therapeutics and Imaging Agents to the Tumour Vasculature. *Drug Resist Update* **2005**, *8*, 381−402.
(57) Yang, H.; Kao, W. J. Synthesis and Characterization of Nanoscale Dendritic Rgd Clusters for Potential Applications in Tissue Engineering and Drug Delivery. *Int. J. Nanomed.* **2007**, *2*, 89−99.
(58) Cai, X.; Li, X.; Liu, Y.; Wu, G.; Zhao, Y.; Chen, F.; Gu, Z. Galactose Decorated Acid-Labile Nanoparticles Encapsulating Quantum Dots for Enhanced Cellular Uptake and Subcellular Localization. *Pharm. Res.* **2012**, *29*, 2167−2179.
(59) Duan, C.; Gao, J.; Zhang, D.; Jia, L.; Liu, Y.; Zheng, D.; Liu, G.; Tian, X.; Wang, F.; Zhang, Q. Galactose-Decorated Ph-Responsive Nanogels for Hepatoma-Targeted Delivery of Oridonin. *Biomacromolecules* **2011**, *12*, 4335−4343.
(60) Lim, D. W.; Yeom, Y. I.; Park, T. G. Poly(Dmaema-Nvp)-B-Peg-Galactose as Gene Delivery Vector for Hepatocytes. *Bioconjugate Chem.* **2000**, *11*, 688−695.
(61) Suriano, F.; Pratt, R.; Tan, J. P. K.; Wiradharma, N.; Nelson, A.; Yang, Y.-Y.; Dubois, P.; Hedrick, J. L. Synthesis of a Family of Amphiphilic Glycopolymers Via Controlled Ring-Opening Polymerization of Functionalized Cyclic Carbonates and Their Application in Drug Delivery. *Biomaterials* **2010**, *31*, 2637−2645.
(62) Han, J. H.; Oh, Y. K.; Kim, D. S.; Kim, C. K. Enhanced Hepatocyte Uptake and Liver Targeting of Methotrexate Using Galactosylated Albumin as a Carrier. *Int. J. Pharm.* **1999**, *188*, 39−47.
(63) Lai, C. H.; Lin, C. Y.; Wu, H. T.; Chan, H. S.; Chuang, Y. J.; Chen, C. T.; Lin, C. C. Galactose Encapsulated Multifunctional Nanoparticle for Hepg2 Cell Internalization. *Adv. Funct. Mater.* **2010**, *20*, 3948−3958.
(64) Xing, T.; Lai, B.; Ye, X. D.; Yan, L. F. Disulfide Core Cross-Linked Pegylated Polypeptide Nanogel Prepared by a One-Step Ring Opening Copolymerization of N-Carboxyanhydrides for Drug Delivery. *Macromol. Biosci.* **2011**, *11*, 962−969.
(65) Xing, T.; Mao, C. Q.; Lai, B.; Yan, L. F. Synthesis of Disulfide-Cross-Linked Polypeptide Nanogel Conjugated with a near-Infrared Fluorescence Probe for Direct Imaging of Reduction-Induced Drug Release. *ACS Appl. Mater. Interfaces* **2012**, *4*, 5662−5672.

DOI: 10.1021/am508291k
ACS Appl. Mater. Interfaces 2015, 7, 2104−2115